Inorg. Chem. **2009**, *48*, 339−349

Anaerobic Photocleavage of DNA in Red Light by Dicopper(II) Complexes of 3,3′-Dithiodipropionic Acid

Debojyoti Lahiri,[†] Tuhin Bhowmick,[‡] Biswarup Pathak,[†] Oottikkal Shameema,[†] Ashis K. Patra,[†] Suryanarayanarao Ramakumar,[‡] and Akhil R. Chakravarty*[,†]

Department of Inorganic and Physical Chemistry and Bioinformatics Center, Department of Physics, Indian Institute of Science, Bangalore 560012, India

Received May 3, 2008

Binuclear copper(II) complexes [{(phen)Cu^{II}}$_2$(μ-dtdp)$_2$] (**1**), [{(dpq)Cu^{II}}$_2$(μ-dtdp)$_2$] (**2**), [{(phen)Cu^{II}}$_2$(μ-az)$_2$] (**3**), and [{(dpq)Cu^{II}}$_2$(μ-az)$_2$] (**4**) and a zinc(II) complex [{(phen)Zn^{II}}$_2$(μ-dtdp)$_2$] (**5**), having 3,3′-dithiodipropionic acid (H_2dtdp), azelaic acid (nonanedioic acid), 1,10-phenanthroline (phen), and dipyrido[3,2-d:2′,3′-f]quinoxaline (dpq), were prepared and characterized by physicochemical methods. Complex **1** has been structurally characterized by X-ray crystallography. The complexes have each metal center bound to a chelating phenanthroline base and two bridging carboxylate ligands giving a square-planar MN_2O_2 coordination geometry. The molecular structure of complex **1** shows two sterically constrained disulfide moieties of the dtdp ligands. The complexes show good binding propensity to calf thymus DNA in the major groove. The photoinduced DNA cleavage activity of the complexes has been studied using 365 nm UV light and 647.1 nm and >750 nm red light under both aerobic and anaerobic conditions. The phen complex **1**, having dtdp ligand, cleaves supercoiled (SC) DNA to its nicked circular (NC) form. The dpq analogue **2** shows formation of a significant quantity of linear DNA resulting from double-strand breaks (dsb) in air. Mechanistic studies reveal the involvement of $HO^{\bullet}$ and $^1O_2$ as the reactive species under an aerobic medium. The dsb of DNA is rationalized from the docking studies on **2**, showing a close proximity of two photosensitizers, namely, the disulfide moiety of dtdp and the quinoxaline ring of dpq to the complementary strands of DNA. The copper(II) complexes of the dtdp ligand cleave SC DNA to its NC form upon exposure to UV or red light under an argon atmosphere. An enhancement of the DNA cleavage activity under argon has been observed upon increasing the concentration of the DMF solvent in the DMF−Tris buffer medium. Theoretical studies suggest the possibility of sulfide anion radical formation from a copper(II)-bound dtdp ligand in >750 nm red light, which further cleaves the DNA. The copper(II) azelate complexes are inactive under similar reaction conditions. The azelate complex of the dpq ligand cleaves DNA in air following the $^1O_2$ pathway. The zinc(II) complex of the dtdp ligand (**5**) does not show any photoinduced DNA cleavage activity in red light.

Introduction

Photoactivated DNA cleavage under visible light irradiation is of importance in nucleic acid chemistry and for medicinal applications in the photodynamic therapy (PDT) of cancer.[1−10] PDT is used as a noninvasive therapeutic treatment of cancer involving a red-light-induced photoexcitation of a drug at the cancer cells, producing reactive oxygen species that causes oxidative cellular damage, leaving the normal cells unaffected.[11−16] The currently used photoactive PDT drugs are porphyrin-based organic dyes requiring molecular oxygen for their activity.[1,3] The basic requirements for PDT are a red light source for better skin penetration ability, a photosensitizer suitable for activation within the PDT window of 620−800 nm, and molecular

* Author to whom correspondence should be addressed. Fax: 91-80-23600683. E-mail: arc@ipc.iisc.ernet.in.
† Department of Inorganic and Physical Chemistry.
‡ Bioinformatics Center, Department of Physics.

(1) Bonnett, R. *Chemical Aspects of Photodynamic Therapy*; Gordon & Breach: London, U.K., 2000.
(2) Detty, M. R.; Gibson, S. L.; Wagner, S. J. *J. Med. Chem.* **2004**, *47*, 3897.
(3) Verma, S.; Watt, G. M.; Mai, Z.; Hasan, T. *Photochem. Photobiol.* **2007**, *83*, 996.
(4) Henderson, B. W.; Busch, T. M.; Vaughan, L. A.; Frawley, N. P.; Babich, D.; Sosa, T. A.; Zollo, J. D.; Dee, A. S.; Cooper, M. T.; Bellnier, D. A.; Greco, W. R.; Oseroff, A. R. *Cancer Res.* **2000**, *60*, 525.

10.1021/ic800806j CCC: $40.75
Published on Web 12/04/2008

oxygen ($^3O_2$) to form reactive oxygen species (ROS). The porphyrinic compounds in PDT are known to form singlet oxygen ($^1O_2$) as the reactive species in a type-II pathway and cause hypoxic cellular conditions.[1] The porphyrinic drugs could become ineffective in the absence of oxygen. It is thus of importance to design and develop new molecular systems of dual functionality with the potential to cleave DNA under both aerobic and anaerobic reaction conditions considering the hypoxic nature of some cancer cells.

Although there are reports on compounds capable of showing anaerobic DNA damage upon irradiation with UV light, compounds showing similar activity in visible light are rare in the literature and are generally restricted to transition metal complexes.[16−22] Zaleski and co-workers have reported anaerobic DNA cleavage by a tris[3-hydroxy-1,2,3-benzotriazine-4(3*H*)-one]iron(III) complex that produces a localized reactive ligand radical intermediate promoted by N_2 release upon photolysis at $\lambda \geq 455$ nm.[19,21] Copper metalloenediynes are known to show anaerobic DNA photocleavage at $\lambda \geq 395$ nm from Bergman cyclization of the enediyne ligand.[20] Turro and co-workers have shown that d^7-d^7 dirhodium(II,II) complexes have the ability to cleave DNA upon photoexposure to visible light by both oxygen-dependent and -independent pathways.[22] Complex *cis*-$[Rh_2(\mu\text{-}O_2CMe)_2(bpy)(dppz)]^{2+}$ is reported to cleave plasmid DNA upon irradiation at $\lambda > 395$ nm, primarily by an oxygen-dependent type-II pathway along with contribution from the oxygen-independent pathway (bpy, 2,2′-bipyridine; dppz, dipyridophenazine).[22] Cellular study on this dirhodium(II,II) complex shows similar cytotoxicity toward human skin cells as known for hematoporphyrin drugs, thus making the dirhodium(II,II) complexes potential PDT agents.[22]

The present work stems from our interest in designing and developing the chemistry of 3d-metal complexes that are capable of cleaving DNA in an oxygen-independent pathway.[23,24] We have shown that copper(II) complexes having a ligand with a disulfide moiety could be photoactivated to generate reactive species to cleave DNA in red light.[23] The binuclear copper(II) complex $[Cu_2(RSSR)_2]$ of dianionic 2-(thioethyl)salicylaldimine shows efficient DNA cleavage activity in the air upon exposure to red light. It also exhibits ∼25% anaerobic cleavage of supercoiled DNA to its nicked circular form at 632.8 nm using a high complex concentration and long photoexposure time (∼3 h). The low cleavage activity of this complex is attributed to its poor binding propensity to DNA in the absence of any DNA binding ligand in the complex. We have now designed new copper(II) complexes having DNA binder phenanthroline bases and a photoactive ligand having a disulfide moiety to significantly enhance the DNA binding and anaerobic DNA cleavage activity within the PDT window. Ternary dicopper(II) complexes having photoinactive azelaic acid (nonanedioic acid, H_2az) and phenanthroline bases (B) are also prepared along with the complexes of formulation $[\{(B)Cu\}_2(\mu\text{-dtdp})_2]$, in which 3,3′-dithiodipropionic acid (dtdp) acts as a photosensitizer. Planar heterocyclic bases (B), namely, 1,10-phenanthroline (phen) and dipyrido[3,2-d:2′,3′-f]quinoxaline (dpq), are chosen for their efficient DNA binding propensity. To explore the role of the d^9-copper(II) ion, a diamagnetic d^{10}-zinc(II) complex having the dtdp ligand is prepared. Herein, we present the synthesis, structure, DNA binding, and photoinduced DNA cleavage activity of $[\{(phen)Cu^{II}\}_2(\mu\text{-dtdp})_2]$ (**1**), $[\{(dpq)Cu^{II}\}_2(\mu\text{-dtdp})_2]$ (**2**), $[\{(phen)Cu^{II}\}_2(\mu\text{-az})_2]$ (**3**), $[\{(dpq)Cu^{II}\}_2(\mu\text{-az})_2]$ (**4**), and $[\{(phen)Zn^{II}\}_2(\mu\text{-dtdp})_2]$ (**5**) (Chart 1). The significant observation of this study is the unprecedented red-light-induced anaerobic DNA cleavage activity of complexes **1** and **2** at $\lambda > 750$ nm. Lutetium texaphyrin (LUTRIN) and phthalocyanin-based PDT drugs are only known to be active near 730 nm under aerobic conditions.[14,15] In addition, complex **2** shows biologically important DNA double-strand breaks (dsb) in the air and

(5) (a) DeRosa, M. C.; Crutchley, R. J. *Coord. Chem. Rev.* **2002**, *233−234*, 351. (b) Ali, H.; van Lier, J. E. *Chem. Rev.* **1999**, *99*, 2379. (c) Sternberg, E. D.; Dolphin, D.; Brückner, C. *Tetrahedron* **1998**, *54*, 4151.

(6) (a) Szacilowski, K.; Macyk, W.; Drzewiecka-Matuszek, A.; Brindell, M.; Stochel, G. *Chem. Rev.* **2005**, *105*, 2647. (b) Armitage, B. *Chem. Rev.* **1998**, *98*, 1171.

(7) (a) Burrows, C. J.; Muller, J. G. *Chem. Rev.* **1998**, *98*, 1109. (b) Sigman, D. S.; Mazumder, A.; Perrin, D. M. *Chem. Rev.* **1993**, *93*, 2295.

(8) Pogozelski, W. K.; Tullius, T. D. *Chem. Rev.* **1998**, *98*, 1089.

(9) (a) Janaratne, T. K.; Yadav, A.; Ongeri, F.; MacDonnell, F. M. *Inorg. Chem.* **2007**, *46*, 3420. (b) Chen, T.; Cook, G. P.; Koppisch, A. T.; Greenberg, M. M. *J. Am. Chem. Soc.* **2000**, *122*, 3861.

(10) (a) Basak, A.; Mandal, S.; Bag, S. S. *Chem. Rev.* **2003**, *103*, 4077. (b) Liang, G.; Wang, L.; Yang, Z.; Koon, H.; Mak, N.; Chang, C. K.; Xu, B. *Chem. Commun.* **2006**, *48*, 5021.

(11) Rodriguez, M. E.; Moran, F.; Bonansea, A.; Monetti, M.; Fernandez, D. A.; Strassert, C. A.; Rivarola, V.; Awruch, J.; Dicelio, L. E. *Photochem. Photobiol. Sci.* **2003**, *2*, 988.

(12) (a) Wei, W.-H.; Wang, Z.; Mizuno, T.; Cortez, C; Fu, L.; Sirisawad, M.; Naumovski, L.; Magda, D.; Sessler, J. L. *Dalton Trans.* **2006**, 1934. (b) Young, S. W.; Woodburn, K. W.; Wright, M.; Mody, T. D.; Fan, Q.; Sessler, J. L.; Dow, W. C.; Miller, R. A. *Photochem. Photobiol.* **1996**, *63*, 892.

(13) (a) Peng, Q.; Warloe, T.; Berg, K.; Moan, J.; Kongshaug, M.; Giercksky, K.-E.; Nesland, J. M. *Cancer* **1997**, *79*, 2282. (b) Kennedy, J. C.; Pottier, R. H.; Pross, D. C. *J. Photochem. Photobiol., B* **1990**, *6*, 143.

(14) (a) Dilkes, M. G.; De Jode, M. L.; Rowntree-Taylor, A. *Lasers Med. Sci.* **1997**, *11*, 23. (b) Bonnett, R.; White, R. D.; Winfield, U.-J.; Berenbaum, M. C. *Biochem. J.* **1989**, *261*, 277. (c) Razum, N.; Snyder, A.; Doiron, D. *Proc. Soc. Photo-opt. Instrum. Eng.* **1996**, *2675*, 43. (d) Morgan, A. R.; Garbo, G. M.; Keck, R. W.; Selman, S. H. *Cancer Res.* **1988**, *48*, 194.

(15) (a) Nelson, J. S.; Roberts, W. G.; Berns, J. W. *Cancer Res.* **1987**, *47*, 4681. (b) Pandey, R. K.; Sumlin, A. B.; Constantine, S.; Aoudia, M.; Potter, W. R.; Bellnier, D. A.; Henderson, B. W.; Rodgers, M. A.; Smith, K. M.; Dougherty, T. J. *Photochem. Photobiol.* **1996**, *64*, 194.

(16) (a) Stranadko, E.; Skobelkin, O.; Litwin, G.; Astrakhankina, T. *Proc. Soc. Photo-opt. Instrum. Eng.* **1994**, *2325*, 240. (b) Richter, A. M.; Kelly, B.; Chow, J.; Liu, D. J.; Towers, G. H. N.; Dolphin, D.; Levy, J. G. *J. Natl. Cancer. Inst.* **1987**, *79*, 1327. (c) Levy, J. G.; Chan, A.; Strong, H. A. *Proc. Soc. Photo-opt. Instrum. Eng.* **1996**, *2625*, 86.

(17) (a) Tanaka, M.; Ohkubo, K.; Fukuzumi, S. *J. Am. Chem. Soc.* **2006**, *128*, 12372. (b) Ohkubo, K.; Yukimoto, K.; Fukuzumi, S. *Chem. Commun.* **2006**, 2504.

(18) Ramaiah, D.; Eckert, I.; Arun, K. T.; Weidenfeller, L.; Epe, B. *Photochem. Photobiol.* **2004**, *79*, 99.

(19) Maurer, T. D.; Kraft, B. J.; Lato, S. M.; Ellington, A. D.; Zaleski, J. M. *Chem. Commun.* **2000**, 69.

(20) (a) Benites, P. J.; Holmberg, R. C.; Rawat, D. S.; Kraft, B. J.; Klein, L. J.; Peters, D. G.; Thorp, H. H.; Zaleski, J. M. *J. Am. Chem. Soc.* **2003**, *125*, 6434.

(21) Bradley, P. M.; Angeles-Boza, A. M.; Dunbar, K. R.; Turro, C. *Inorg. Chem.* **2004**, *43*, 2450.

(22) (a) Angeles-Boza, A. M.; Bradley, P. M.; Fu, P. K.-L.; Shatruk, M.; Hilfiger, M. G.; Dunbar, K. R.; Turro, C. *Inorg. Chem.* **2005**, *44*, 7262. (b) Angeles-Boza, A. M.; Bradley, P. M.; Fu, P. K.-L.; Wicke, S. E.; Bacsa, J.; Dunbar, K. R.; Turro, C. *Inorg. Chem.* **2004**, *43*, 8510.

(23) Dhar, S.; Nethaji, M.; Chakravarty, A. R. *Dalton Trans.* **2005**, 344.

(24) Dhar, S.; Nethaji, M.; Chakravarty, A. R. *Dalton Trans.* **2004**, 4180.

Chart 1. Ternary Complexes **1**−**5** and the Phenanthroline Bases

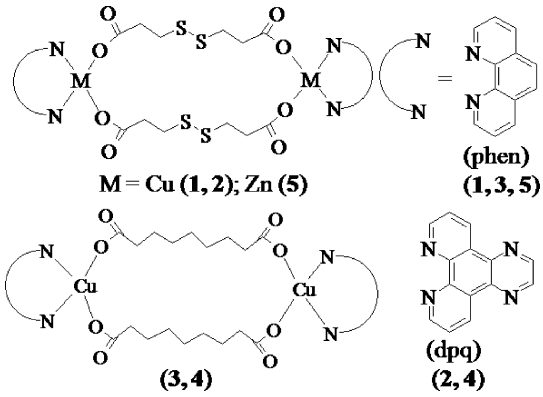

DNA single-strand breaks (ssb) under argon, making it active under both aerobic and hypoxic conditions. The DNA binding and photoinduced DNA cleavage properties of the complexes are rationalized from DNA docking and computational studies.

Experimental Section

Materials and Methods. All reagents and chemicals were purchased from commercial sources and used as received without further purification. Solvents used for electrochemistry and spectroscopic measurements were purified by standard procedures.[25] Supercoiled (SC) pUC19 DNA (cesium chloride purified) was procured from Bangalore Genie (India). Calf thymus (CT) DNA, agarose (molecular biology grade), distamycin, 5,5-dimethyl-1-pyrroline *N*-oxide (DMPO), catalase, methyl green, ethidium bromide (EB), and superoxide dismutase (SOD) were from Sigma (USA). Tris(hydroxymethyl)aminomethane−HCl (Tris−HCl) buffer was prepared using deionized and sonicated triple-distilled water. Complex $[\{(phen)Cu\}_2(\mu\text{-}az)_2]$ (**3**) and ligand dpq were prepared following literature methods.[26,27] The phen and dtdp were purchased from Aldrich (USA).

The elemental analysis was done using a Thermo Finnigan FLASH EA 1112 CHNS analyzer. The infrared and electronic spectra were recorded on Perkin-Elmer Lambda 35 and Varian Cary 300 Bio machines, respectively, at 25 °C. Variable-temperature magnetic susceptibility data (300−20 K) for the polycrystalline samples of the complexes were obtained using the Model 300 Lewis-coil-force magnetometer made by George Associates Inc. (Berkeley, CA). $Hg[Co(NCS)_4]$ was used as a standard. Experimental susceptibility data were corrected for diamagnetic contributions.[28] The molar magnetic susceptibilities were fitted by Bleaney−Bowers expression by means of a least-squares program: $\chi_{Cu} = [Ng^2\beta^2/kT][3 + \exp(-2J/kT)]^{-1} + N_\alpha$.[28] Electrochemical measurements were made at 25 °C on an EG&G PAR model 253 VersaStat potentiostat/galvanostat with electrochemical analysis software 270, using a three-electrode setup comprised of a glassy carbon working electrode, platinum wire auxiliary electrode, and saturated calomel reference electrode (SCE) in DMF−Tris−HCl buffer (2:1 v/v). Tetrabutylammonium perchlorate (TBAP, 0.1 M) was used as a supporting electrolyte for the electrochemical measurements. Mass spectral measurements were done in aqueous DMF on an LC-ESI MS model ESQuire 3000 plus machine (Bruker Daltonics, Germany).

Preparation of $[\{(B)Cu^{II}\}_2(\mu\text{-dtdp})_2]$ (B = phen, 1; dpq, 2). The binuclear copper(II) complexes **1** and **2** were prepared in ∼70% yield following a general procedure in which copper(II) acetate hydrate (0.2 g, 1.0 mmol) in methanol (5 mL) was reacted with a methanol solution (10 mL) of the heterocyclic base [phen, 0.2 g (1.0 mmol); dpq, 0.23 g (1.0 mmol)] followed by the addition of a methanol solution (15 mL) of 3,3′-dithiodipropionic acid (0.21 g, 1.0 mmol). The reaction mixture was stirred for 7 h at 25 °C. The solution was filtered, and the filtrate on slow evaporation gave the blue-colored product. The solid was isolated and washed with cold aqueous methanol and dried over P_4O_{10} (Yield: **1**, 0.32 g; **2**, 0.36 g). Anal. calcd for $C_{36}H_{32}Cu_2N_4O_8S_4$ (**1**): C, 47.83; H, 3.57; N, 6.20. Found: C, 47.94; H, 3.64; N, 6.36. IR (KBr phase): 3435br, 3053m, 1614vs, 1522m, 1430m, 1380s, 1296m, 1205s, 1108m, 1049w, 986w, 936w, 852s, 782w, 717m, 675m cm^{-1} [br, broad; vs, very strong; s, strong; m, medium; w, weak]. UV−visible in 1:1 DMF−water [λ/nm (ε/ M^{-1} cm^{-1})]: 273 (49250), 294 (16500), 672 (320). Molar conductance in 1:1 DMF−water at 25 °C (Λ_M/ S m^2 M^{-1}): 21. $\mu_{eff} = 1.74$ μ_B (per copper) at 298 K. ESI-MS in aqueous DMF: 905.0 *m*/*z*. Anal. calcd for $C_{40}H_{36}Cu_2N_8O_8S_4$ (**2**): C, 47.66; H, 3.20; N, 11.12. Found: C, 47.56; H, 3.48; N, 11.05. IR (KBr phase): 3396br, 3073m, 1573vs, 1486s, 1402s, 1385s, 1311s, 1281s, 1218m, 1138m, 1079m, 932w, 828m, 732s, 679m, 436w cm^{-1}. UV−visible in 1:1 DMF−water [λ/nm (ε/M^{-1} cm^{-1})]: 258 (67200), 296 (23250), 661 (120). Molar conductance in 1:1 DMF−water at 25 °C (Λ_M/ S m^2 M^{-1}): 20. $\mu_{eff} = 1.77$ μ_B (per copper) at 298 K. ESI-MS in aqueous DMF: 1008.6 *m*/*z*.

Preparation of $[\{(dpq)Cu\}_2(\mu\text{-az})_2]$ (4). Complex **4** was prepared in ∼70% yield from a reaction of copper(II) acetate hydrate (0.2 g, 1.0 mmol) in methanol (5 mL) with a methanol solution (10 mL) of dipyridoquinoxaline (0.23 g, 1.0 mmol) and a methanol solution (15 mL) of azelaic acid (0.17 g, 1.0 mmol). The reaction mixture after stirring for 7 h at 25 °C was filtered, and the filtrate on slow evaporation gave a blue-colored solid that was isolated and washed with cold aqueous methanol and finally dried in a vacuum over P_4O_{10} (Yield for **4**: 0.34 g). Anal. calcd for $C_{46}H_{48}Cu_2N_8O_8$ (**4**): C, 57.31; H, 4.60; N, 11.62. Found: C, 57.14; H, 4.38; N, 11.53. IR (KBr phase): 3370br, 2933m, 2854m, 1718w, 1601vs, 1486s, 1463m, 1407s, 1385s, 1278m, 1209m, 1082m, 884w, 816s, 729m, 672w, 609w, 427m cm^{-1}. UV−visible in 1:1 DMF−water [λ/nm (ε/M^{-1} cm^{-1})]: 273 (49350), 294 (15670), 669 (90). Molar conductance in 1:1 DMF−water at 25 °C (Λ_M/S m^2 M^{-1}): 22. $\mu_{eff} = 1.75$ μ_B (per copper) at 298 K. ESI-MS in aqueous DMF: 963.2 *m*/*z*.

Preparation of $[\{(phen)Zn\}_2(\mu\text{-dtdp})_2]$ (5). The zinc(II) complex was prepared in ∼75% yield from the reaction of a methanol solution (8 mL) of 1,10-phenanthroline (0.2 g, 1.0 mmol) with an aqueous solution (10 mL) of 3,3′-dithiodipropionic acid (0.21 g, 1.0 mmol) and zinc(II) acetate dihydrate (0.22 g, 1.0 mmol). After stirring for 30 min, the white solid was filtered off, washed with cold aqueous methanol, and dried in a vacuum over P_4O_{10} (Yield for **5**: 0.35 g). Anal. calcd for $C_{36}H_{32}Zn_2N_4O_8S_4$ (**5**): C, 47.62; H, 3.55; N, 6.17. Found: C, 47.44; H, 3.46; N, 5.97. IR (KBr phase): 3403br, 2920w, 1581s, 1520s, 1402s, 1305s, 1277m, 1197w, 1138w, 1105w, 932w, 852s, 725s, 666m, 588m, 424w cm^{-1}. UV−visible in water [λ/nm (ε/$M^{-1}cm^{-1}$)]: 269 (19750), 292 (7150). Molar conductance in 1:1 DMF−water at 25 °C (Λ_M/S m^2 M^{-1}): 20. ESI-MS in water: 908.9 *m*/*z*.

(25) Perrin, D. D.; Armarego, W. L. F.; Perrin, D. R. *Purification of Laboratory Chemicals*; Pergamon Press: Oxford, U.K., 1980.
(26) Zheng, Y.-Q.; Sun, J.; Lin, J.-L. *Z. Anorg. Allg. Chem.* **2000**, *626*, 1271.
(27) (a) Dickeson, J. E.; Summers, L. A. *Aus. J. Chem.* **1970**, *23*, 1023. (b) Collins, J. G.; Sleeman, A. D.; Aldrich-Wright, J. R.; Greguric, I.; Hambley, T. W *Inorg. Chem.* **1998**, *37*, 3133.
(28) (a) Kahn, O. *Molecular Magnetism*; VCH: Weinheim, Germany, 1993. (b) Bleaney, B.; Bowers, K. D. *Proc. R. Soc. London, Ser. A* **1952**, *214*, 451.

Table 1. Selected Crystallographic Data for $[\{(phen)Cu\}_2(\mu\text{-dtdp})_2]\cdot 2H_2O$ (**1**·2H$_2$O)

formula	$C_{36}H_{36}Cu_2N_4O_{10}S_4$
fw, g M^{-1}	940.01
cryst syst	triclinic
space group (no.)	$P\bar{1}$ (2)
a, Å	10.007(3)
b, Å	10.415(3)
c, Å	10.684(3)
α, deg	69.032(6)
β, deg	82.108(6)
γ, deg	72.608(5)
V, Å^3	991.7(5)
Z	1
T, K	293(2)
ρ_{calcd}, g cm^{-3}	1.574
λ, Å (Mo Kα)	0.71073
μ, cm^{-1}	13.44
data/restraints/params	3882/0/253
goodness-of-fit on F^2	1.051
R (F_o)[a] ($I > 2\sigma(I)$) [R all data]	0.0875 [0.1511]
wR (F_o)[b] ($I > 2\sigma(I)$) [wR (all data)]	0.1638 [0.1904]
largest diff. peak and hole (e Å^{-3})	0.947, −0.377
$w = 1/[\sigma^2(F_o^2) + (AP)^2 + (BP)]$	A = 0.0821; B = 0.0

[a] $R = \sum||F_o|| - ||F_c||/\sum||F_o||$. [b] $wR = \{\sum[w(F_o^2 - F_c^2)^2]/\sum[w(F_o)^2]\}^{1/2}$, $w = [\sigma^2(F_o)^2 + (AP)^2 + BP]^{-1}$, $P = (F_o^2 + 2F_c^2)/3$.

Solubility and Stability. The copper(II) complexes were soluble in aqueous DMF and insoluble in hydrocarbons. The zinc(II) complex showed good solubility in water and polar organic solvents. The complexes were stable in aqueous DMF and in the Tris−HCl buffer.

X-Ray Crystallographic Procedure. Single crystals of $[\{(phen)Cu\}_2(\mu\text{-dtdp})_2]$ (**1**) were obtained upon slow evaporation of the reaction mixture of the complex. Crystal mounting was done on a glass fiber with epoxy cement. All geometric and intensity data were collected at room temperature using an automated Bruker SMART APEX CCD diffractometer equipped with a fine-focus 1.75 kW sealed-tube Mo Kα X-ray source (λ = 0.71073 Å) with increasing ω (width of 0.3° per frame) at a scan speed of 19 s/frame. The intensity data were corrected for Lorentz-polarization effects and for absorption.[29] The structure was solved and refined with the SHELX system of programs.[30] The hydrogen atoms were fixed in their calculated positions and refined using a riding model. All non-hydrogen atoms were refined anisotropically. Selected crystal data for the complex are summarized in Table 1. A perspective view of the molecule was obtained by ORTEP.[31]

DNA Binding Experiments. The DNA binding experiments were done in a Tris−HCl buffer (5 mM, pH 7.2) using the complex solution in DMF. The CT DNA (ca. 350 μM NP) in the buffer medium showed a ratio of the UV absorbance at 260 and 280 nm of ca. 1.9:1, indicating that the DNA was apparently free from protein. The concentration of CT DNA was estimated from its absorption band intensity at 260 nm with a known molar absorption coefficient value of 6600 M^{-1} cm^{-1}.[32] Absorption titration experiments were done by varying the concentration of the CT DNA, keeping the complex concentration constant. Due correction was made for the absorbance of DNA itself, and all of the UV spectra were recorded after equilibration. The intrinsic equilibrium DNA binding constants (K_b) along with binding site sizes (s) of the complexes to CT DNA were determined by monitoring the change of the absorption intensity of the spectral bands with increasing concentration of the CT DNA by regression analysis using the following equation: $(\varepsilon_a - \varepsilon_f)/(\varepsilon_b - \varepsilon_f) = (b - (b^2 - 2K_b^2C_t[DNA]/s)^{1/2})/2K_bC_t$, where $b = 1 + K_bC_t + K_b[DNA]_t/2s$, ε_a is the extinction coefficient observed for the charge-transfer absorption band at a given DNA concentration, ε_f is the extinction coefficient of the complex free in solution, ε_b is the extinction coefficient of the complex when fully bound to DNA, K_b is the equilibrium binding constant, C_t is the total metal complex concentration, [DNA] is the DNA concentration in nucleotides, and s is the binding site size in base pairs.[33,34] The nonlinear least-squares analysis was done using Origin Laboratory, version 7.5.

DNA-melting experiments were carried out by monitoring the absorbance (λ = 260 nm) of CT-DNA (150 μM NP) at various temperatures in the absence and presence of the complexes in a 2:1 ratio of DNA and complex, with a ramp rate of 0.5 °C/min in a phosphate buffer (pH 6.85) using a Peltier system attached to the UV−visible spectrophotometer. Viscometric titrations were done using a Schott Gerate AVS 310 Automated Viscometer thermostatted at 37 °C in a constant temperature bath. The concentration of CT DNA was 162 μM in NP, and the flow times were measured with an automated timer. Each sample was measured three times, and an average flow time was calculated. The relative solution viscosity (η/η_0) was estimated from the relation $(L/L_0) = (\eta/\eta_0)^{1/3}$, where (L/L_0) is the contour length and L_0 and η_0 denote the apparent molecular length and solution viscosity, respectively, in the absence of the metal complex.[35] The viscosity data were presented as $(\eta/\eta_0)^{1/3}$ versus [complex]/[DNA], where η is the viscosity of DNA in the presence of the complex and η_0 that of DNA alone. Viscosity values were obtained from the observed flowing time of DNA-containing solutions (t) corrected for that of the buffer alone (t_0), $\eta = t - t_0$.

DNA Photocleavage Experiments. The photoinduced cleavage of SC pUC19 DNA by the copper(II) and zinc(II) complexes was studied by the agarose gel electrophoresis method. The reactions were carried out under illuminated conditions using a UV lamp of 365 nm (6 W, sample area of illumination 45 mm^2, Bangalore Genie make) and in 647.1 and >750 nm red light using a continuous-wave (CW) Ar−Kr mixed-gas ion laser (100 mW, laser beam diameter 1.8 mm, beam divergence 0.70 mrad, Spectra Physics Water-Cooled Mixed-Gas Ion Laser Stabilite 2018-RM) fitted with a model 2018-RM-IR IR attachment with all-lines IR optics (752.5−799.3 nm). The power of the laser beam was measured using a Spectra Physics CW Laser Power Meter (Model 407A). Eppendorf and glass vials were used for respective UV and visible light experiments in a dark room at 25 °C using SC DNA (1 μL, 30 μM) in a 50 mM Tris-(hydroxymethyl)methane−HCl (Tris−HCl) buffer (pH 7.2) containing 50 mM NaCl and the complex (2 μL in DMF) with varied concentrations. The concentration of the complexes in DMF or the additives in the buffer corresponded to the quantity after dilution of the 2 μL stock solution to the 20 μL final volume using the Tris−HCl buffer. The solution path length used for illumination in the sample vial was ∼5 mm.

The sample after the photoexposure was incubated for 1 h at 37 °C, followed by its addition to the loading buffer containing 25% bromophenol blue, 0.25% xylene cyanol, and 30% glycerol (3 μL), and the solution was finally loaded on 0.8% agarose gel containing 1.0 μg mL^{-1} ethidium bromide. The electrophoresis was carried

(29) Walker, N.; Stuart, D. *Acta Crystallogr.* **1983**, *A39*, 158.
(30) Sheldrick, G. M. *SHELX-97*; University of Göttingen: Göttingen, Germany, 1997.
(31) Burnett, M. N., III. *Report ORNL-6895*, Oak Ridge National Laboratory: Oak Ridge, TN, 1996.
(32) Reichman, M. E.; Rice, S. A.; Thomas, C. A.; Doty, P. *J. Am. Chem. Soc.* **1954**, *76*, 3047.
(33) McGhee, J. D.; von Hippel, P. H. *J. Mol. Biol.* **1974**, *86*, 469.
(34) Carter, M. T.; Rodriguez, M.; Bard, A. J. *J. Am. Chem. Soc.* **1989**, *111*, 8901.
(35) Cohen, G.; Eisenberg, H. *Biopolymers* **1969**, *8*, 45.

out in a dark room for 2 h at 50 V in a TAE (Tris−acetate−EDTA) buffer. The bands were visualized by UV light and photographed. The extent of cleavage of SC DNA was measured from the intensities of the bands using a UVITECH Gel Documentation System. Due corrections were made for the low level of nicked circular (NC) DNA present in the original SC DNA sample and for the low affinity of EB binding to SC compared to NC and linear forms of DNA.[36] The error range observed in determining the band intensities was ±3−5%. Different additives (distamycin, 100 μM; methyl green, 200 μM; DMSO, 4 μL; sodium azide, 100 μM; catalase, four units; SOD, four units) were added to the SC DNA for mechanistic studies prior to light exposure. For the D_2O experiment, this solvent was used for dilution of the sample to 20 μL.

Computational Procedures. The molecular docking calculations on complex **2** were done using the Discovery Studio (DS) Modeling 1.2-SBD Docking Module by Accelrys Software.[37] The CHARMm force field was assigned to the metal complex in the input of the calculations. Due to higher coordination of the copper(II) in the complexes, correction of the partial charge distribution for all of the atoms in the complex was made by following the output from Gaussian 03.[38] The energy-minimized structure of complex **2** was generated from the coordinates of the crystallographic structure of complex **1**. Model building and optimization were done using the DS Modeling 1.1 SBD model building and energy minimization modules of the Accelrys software package to get insights into the binding aspects of the complexes to the double-stranded DNA. After making the necessary changes, the model was subjected to energy minimization via conjugate gradient steps. The crystal structure of the B-DNA dodecamer d(CGCGAATTCGCG)$_2$ (PDB ID:355D) was downloaded from the protein data bank (PDB). In the docking analysis, the binding site was assigned across all of the minor and major grooves of the DNA molecule. As the docking module primarily imparted flexibility of the complex and considered the receptor macromolecule as a rigid entity, to impart partial flexibility to the docking site of the receptor (DNA), local distortion in the intercalation site was enhanced using the program NAMOT to provide a more realistic docking environment.[39] The docking was performed to find the most stable and favorable orientation. The docking options consisted of the following steps: (i) Monte Carlo options to perform a flexible fit, (ii) thresholds for diversity of the saved pose (defined to 2 Å to scan through different conformations), (iii) pose optimization done in two steps, (a) steepest descent minimization and (b) BFGS rigid body minimization, (iv) ligand internal energy optimization and filtering of poses with short contacts (VDW and electrostatic energy calculated), and (v) pose filtering and processing. Dock scores for conformations above energy 2.0 kcal M^{-1} were accepted. Clustering of poses using a leader algorithm was done. Scoring for the docked poses was determined primarily using a Ludi score that included five major contributions due to (a) ideal hydrogen bonds, (b) perturbed ionic interaction, (c) lipophilic interaction, (d) the freezing of internal degrees of freedom, and (e) loss of translational and rotational entropy of the ligand. The optimum docking state with the highest energy stabilization was obtained in a two stage docking. After the initial docking, a thorough analysis of different docked poses and the corresponding conformations of the metal complexes were done. The best binding trends using the top-scored conformations of the complex obtained in the first stage docking were taken as input for the second stage of docking. DFT calculations (B3LYP/LANL2DZ) on [{(phen)Cu}$_2$(μ-dtdp)$_2$] (**1**) were carried out using the G03 program to get insight on the R−S−S−R bond cleavage pathway(s).[38,40] Considering the large number of atoms in the complex, only single-point calculations on the crystallographic structure were done. Accurate S−S bond dissociation energies were calculated and supported by theoretical approaches.[41]

Results and Discussion

Synthesis and General Aspects. On the basis of our objective to design new copper(II) complexes that are capable of showing efficient anaerobic DNA cleavage activity in red light, we have chosen dtdp as a photosensitizer and phenanthroline bases, namely, phen and dpq, as DNA binders. The dpq ligand with its quinoxaline moiety could act as a photosensitizer generating $^3(n-\pi^*)$ and $^3(\pi-\pi^*)$ state(s).[42] Binuclear copper(II) complexes [{(phen)Cu}$_2$(μ-dtdp)$_2$] (**1**), [{(dpq)Cu}$_2$(μ-dtdp)$_2$] (**2**), [{(phen)Cu}$_2$(μ-az)$_2$] (**3**), and [{(dpq)Cu}$_2$(μ-az)$_2$] (**4**) and a zinc(II) complex [{(phen)Zn}$_2$(μ-dtdp)$_2$] (**5**) were prepared in high yields and characterized by physicochemical methods (Chart 1, Table 2). The azelate (az) complexes **3** and **4** were prepared to explore the role of the disulfide moiety in dtdp on the DNA cleavage activity of **1** and **2**. The zinc(II) complex **5** was prepared for mechanistic studies to understand the role of 3d-metal in the photoinduced DNA cleavage activity of the complexes.

The infrared spectra of the complexes show a characteristic band of the dtdp and azelate ligands near 1600 cm^{-1} assignable to the carbonyl (C═O) stretch of the carboxylate moiety. The binuclear complexes are found to be stable in the solution phase, as evidenced by the mass spectral data (Figures S1−S5, Supporting Information). Complexes **1**−**5** are essentially nonelectrolytic in nature, showing a molar conductance value of ∼20 S m^2 M^{-1} in aqueous DMF. The copper(II) complexes show a visible band in the PDT window of 620−800 nm in aqueous DMF (Figure 1, Figure S6, Supporting Information). Variable-temperature magnetic

(36) Bernadou, J.; Pratviel, G.; Bennis, F.; Girardet, M.; Meunier, B. *Biochemistry* **1989**, *28*, 7268.
(37) *Structure-Based Drug Design with Discovery Studio, Accelrys, version 0406*; Accelrys Software Inc.: San Diego, CA, 2003.
(38) Frisch, M. J.; Trucks, G. W.; Schlegel, H. B.; Scuseria, G. E.; Robb, M. A.; Cheeseman, J. R.; Montgomery, J. A., Jr.; Vreven, T.; Kudin, K. N.; Burant, J. C.; Millam, J. M.; Iyengar, S. S.; Tomasi, J.; Barone, V.; Mennucci, B.; Cossi, M.; Scalmani, G.; Rega, N.; Petersson, G. A.; Nakatsuji, H.; Hada, M.; Ehara, M.; Toyota, K.; Fukuda, R.; Hasegawa, J.; Ishida, M.; Nakajima, T.; Honda, Y.; Kitao, O.; Nakai, H.; Klene, M.; Li, X.; Knox, J. E.; Hratchian, H. P.; Cross, J. B.; Adamo, C.; Jaramillo, J.; Gomperts, R.; Stratmann, R. E.; Yazyev, O.; Austin, A. J.; Cammi, R.; Pomelli, C.; Ochterski, J. W.; Ayala, P. Y.; Morokuma, K.; Voth, G. A.; Salvador, P.; Dannenberg, J. J.; Zakrzewski, V. G.; Dapprich, S.; Daniels, A. D.; Strain, M. C.; Farkas, O.; Malick, D. K.; Rabuck, A. D.; Raghavachari, K.; Foresman, J. B.; Ortiz, J. V.; Cui, Q.; Baboul, A. G.; Clifford, S.; Cioslowski, J.; Stefanov, B. B.; Liu, G.; Liashenko, A.; Piskorz, P.; Komaromi, I.; Martin, R. L.; Fox, D. J.; Keith, T.; Al-Laham, M. A.; Peng, C. Y.; Nanayakkara, A.; Challacombe, M.; Gill, P. M. W.; Johnson, B.; Chen, W.; Wong, M. W.; Gonzalez, C.; Pople, J. A. *Gaussian 03*, revision C.2; Gaussian, Inc.: Wallingford, CT, 2004.
(39) *NAMOT: Nucleic Acid Modeling Tool*; Theoretical Biology and Biophysics (T-10), Theoretical Division, Los Alamos National Laboratory: Los Alamos, NM.
(40) (a) Becke, A. D. *Phys. Rev. A: At., Mol., Opt Phys.* **1988**, *38*, 3098. (b) Lee, C.; Yang, W.; Parr, R. G. *Phys. Rev. B: Condens. Matter Mater. Phys.* **1988**, *37*, 785.
(41) (a) Nourbakhsh, S.; Liao, C.-L.; Ng, C. Y. *J. Chem. Phys.* **1990**, *92*, 6587. (b) Benassi, R.; Taddei, F. *J. Phys. Chem. A* **1998**, *102*, 6173. (c) Fournier, R.; De Pristo, A. E. *J. Chem. Phys.* **1992**, *96*, 1183.
(42) Toshima, K.; Takano, R.; Ozawa, T.; Matsumara, S. *Chem. Commun.* **2002**, 212.

Table 2. Physicochemical Data and the DNA Binding Parameters for Complexes **1**−**5**

complex	λ, nm (ε, M^{-1} cm^{-1})[a]	$E_{1/2}$, V (ΔE_p, mV)[b]	μ_{eff},[c] μ_B ($-2J$, cm^{-1})	ΔT_m[d]/°C	K_b/M^{-1} [s][e]	Λ_M[f]/S m^2 M^{-1}
[{(phen)Cu}$_2$(μ-dtdp)$_2$] (**1**)	672 (320)	0.08 (320)	1.74 (0.1)	2.1	3.3 (±0.7) × 10^5 [0.3]	21
[{(dpq)Cu}$_2$(μ-dtdp)$_2$] (**2**)	661 (120)	0.11 (350)	1.77 (1.2)	4.2	4.1 (±0.9) × 10^6 [0.8]	20
[{(phen)Cu}$_2$(μ-az)$_2$] (**3**)	668 (95)	−0.09 (260)	1.78 (0.6)	2.0	2.2 (±0.5) × 10^5 [0.5]	23
[{(dpq)Cu}$_2$(μ-az)$_2$] (**4**)	669 (90)	−0.15 (300)	1.75 (0.9)	4.3	1.8 (±0.5) × 10^6 [0.8]	22
[{(phen)Zn}$_2$(μ-dtdp)$_2$] (**5**)				2.3	1.5 (±0.5) × 10^5 [0.4]	20

[a] Visible band in DMF−Tris buffer (1:1 v/v). [b] The Cu(II)/Cu(I) couple at 50 mV s^{-1} in DMF−Tris buffer (1:1 v/v)/0.1 M TBAP. $E_{1/2} = 0.5(E_{pa} + E_{pc})$. $\Delta E_p = |E_{pa} - E_{pc}|$, where E_{pa} and E_{pc} are anodic and cathodic peak potentials, respectively. [c] Magnetic moment per copper. [d] Change in DNA melting temperature. [e] K_b, the DNA binding constant (s, binding site size). [f] Molar conductance value in DMF−water (1:1 v/v) at 25 °C.

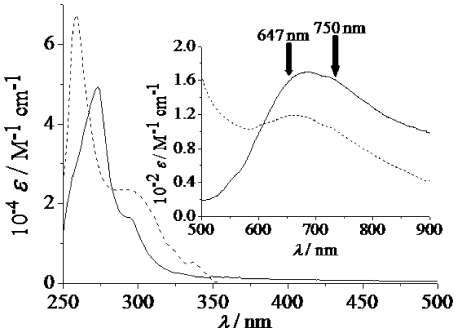

Figure 1. Electronic spectra of [{(phen)Cu}$_2$(μ-dtdp)$_2$] (**1**) (—) and [{(dpq)Cu}$_2$(μ-dtdp)$_2$] (**2**) (---) in aqueous DMF. The photoirradiation wavelengths are shown with an arrow.

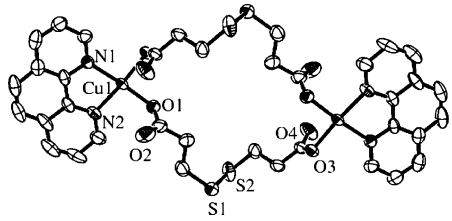

Figure 2. ORTEP view of the complex in [{(phen)Cu}$_2$(μ-dtdp)$_2$]·2H_2O (**1**·2H_2O) showing 50% probability thermal ellipsoids and the atom labeling scheme for the metal and hetero atoms.

susceptibility measurements on the solid powder samples of complexes **1**−**4** show the one-electron paramagnetic nature of each copper(II) center. Theoretical fittings of the susceptibility data gave $-2J$ values that range within 0.1−1.2 cm^{-1}, indicating the essentially noninteracting nature of the copper(II) centers in these complexes (Figure S7, Supporting Information).[28] The copper(II) complexes are redox-active and display one quasireversible cyclic voltammetric response assignable to the Cu(II)/Cu(I) couple in the range of +0.11 to −0.15 V versus SCE in the DMF−Tris−HCl buffer (Figure S8, Supporting Information).

Crystal Structure. Complex **1** has been structurally characterized by single-crystal X-ray crystallography. A perspective view of the complex is shown in Figure 2. The bond distance and bond angle data are presented in Table S1 (Supporting Information). Complex **1** crystallizes in the $P\bar{1}$ space group belonging to the triclinic crystal system with half a molecule and one lattice water in the crystallographic asymmetric unit (Figure S9, Supporting Information). The crystal structure shows that each copper atom is coordinated to a chelating N,N-donor phen and two bridging dithiodipropionato ligands through the carboxylate oxygen, giving a square-planar CuN_2O_2 coordination. The av. Cu−N and Cu−O bond distances are 2.01 and 1.981 Å, respectively. The sulfur atoms of two disulfide units do not show any

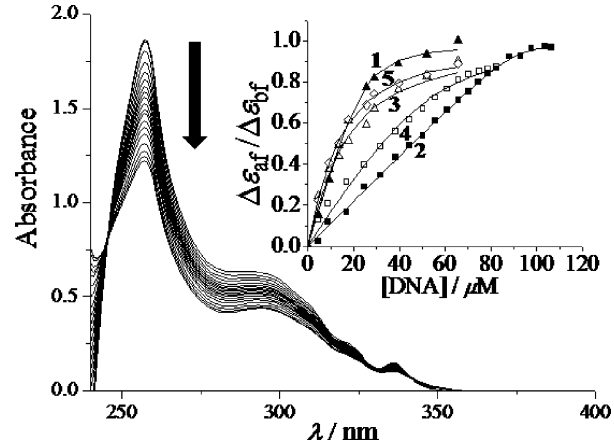

Figure 3. Absorption spectral traces of [{(dpq)Cu}$_2$(μ-dtdp)$_2$] (**2**) with increasing DNA concentration (shown with an arrow). The inset shows the least-squares fit of $\Delta\varepsilon_{af}/\Delta\varepsilon_{bf}$ vs [DNA] for the complexes **1**−**5**.

apparent interaction with the metal centers. The disulfide units are sterically constrained, possibly due to the large size of the sulfur atom. The lattice water molecule shows hydrogen bonding with the carboxylate oxygen of the dtdp ligand, giving a O(2)···O(5) distance of 2.751 Å. The dtdp and azelate complexes differ significantly in their molecular structures, as two azelate ligands in the reported crystal structure of complex **3** do not show any steric crowding.[26]

DNA Binding. The binding of the complexes to calf thymus DNA has been studied by spectral and hydrodynamic techniques, namely, absorption, DNA thermal denaturation, and viscosity measurements (Table 2). We have used the absorption spectral technique to determine the intrinsic binding constant and the binding site size to CT DNA by monitoring the absorption intensity of the charge-transfer spectral band near 300 nm with increasing concentration of the CT-DNA, keeping the complex concentration constant. A complex bound to DNA through intercalation generally causes hypochromism and a red shift (bathochromism) of the absorption band due to strong stacking interactions between the aromatic chromophore of the complex and the base pairs of DNA.[43] The present complexes show only minor hypochromism and a minor shift of the band (~2 nm), indicating the nonintercalating nature of the complexes (Figure 3). The K_b values obtained from the absorption spectral technique are ~10^6 M^{-1}. The phen complexes (**1** and **3**) show moderate binding to CT-DNA, while the dpq analogues (**2** and **4**) are better DNA binders due to the presence of planar quinoxaline rings. The ternary complexes

(43) (a) Gunther, L. E.; Yong, A. S. *J. Am. Chem. Soc.* **1968**, *90*, 7323. (b) An, Y.; Liu, S.-D.; Deng, S.-Y.; Ji, L.-N.; Mao, Z.-W. *J. Inorg. Biochem.* **2006**, *100*, 1586.

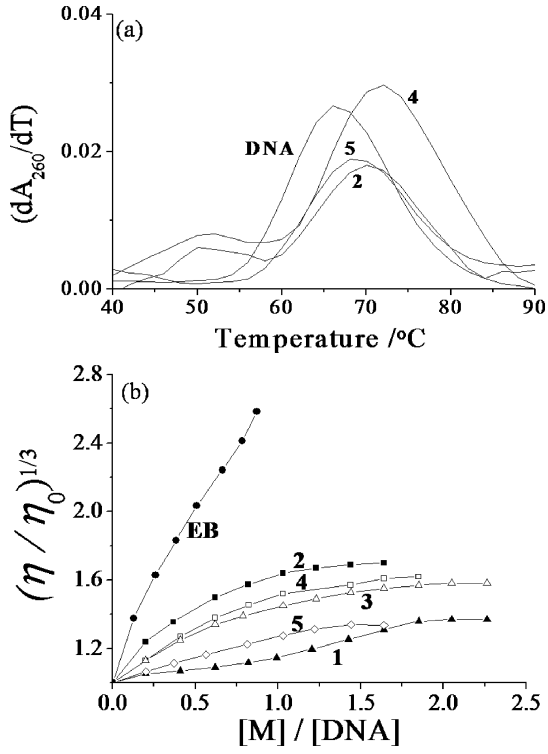

Figure 4. (a) Thermal denaturation plots of 150 μM CT DNA alone and in the presence of the complexes [{(dpq)Cu}$_2$(μ-dtdp)$_2$] (**2**), [{(dpq)Cu}$_2$(μ-az)$_2$] (**4**), and [{(dpq)Zn}$_2$(μ-dtdp)$_2$] (**5**). (b) Effect of increasing the concentration of the complexes **1** (▲), **2** (■), **3** (Δ), **4** (□), **5** (◇), and ethidium bromide (●) on the relative viscosities of CT-DNA at 37.0 (±0.1) °C in 5 mM Tris−HCl buffer (pH, 7.2, CT DNA = 160 μM).

1−**4** are significantly better binders to CT DNA than their binary dicopper(II) analogue [Cu(RSSR)]$_2$ which lacks any DNA binding phenanthroline base.[23,24] The fitted binding site values (*s*) of 0.3 to 0.8 indicate less association of the complexes to the number of DNA bases, suggesting a primarily surface or groove binding nature of the complexes.

Thermal behavior of the DNA in the presence of metal complexes can give insight into their conformational changes and information about the interaction strength with DNA. Thermal studies have shown an increase in the melting temperature (ΔT_m) of CT DNA of ∼2−4 °C upon addition of the complexes. Such a minor change suggests a primarily groove binding nature of the complexes (Table 2, Figure 4).[44] Viscosity measurements have been made to understand the mode of binding of the complexes to DNA. Intercalation of a species into DNA base pairs generally causes a significant increase in the viscosity of the DNA solution due to an increase in the separation of the base pairs to accommodate the bound species, as is evidenced with a classical DNA intercalator, namely, ethidium bromide (Figure 4b).[45,46] In contrast, groove binding or partial intercalation leads to only minor change in the viscosity. The plot of relative specific viscosity $(\eta/\eta_0)^{1/3}$ versus the [complex]/[DNA] ratio shows minor changes in the viscosity for complexes **1**−**5** (Figure 4). The results indicate the groove-binding propensity of the complexes without changing any DNA conformation.

Photocleavage of DNA. The photoinduced DNA cleavage activity of the complexes has been studied under both aerobic and anaerobic conditions using SC pUC19 DNA in a medium of Tris−HCl/NaCl buffer upon photoirradiation at 365 nm UV-A light and 647.1 nm and >750 nm red light (Table 3, Figures 5 and 6, and Figures S10−S12, Supporting Information). The binuclear copper(II) complexes do not show any significant DNA cleavage activity in the dark. When exposed to light, complex **1**, having phen and dtdp, shows DNA cleavage activity forming NC DNA, while its azelate analogue **3** is cleavage-inactive. Complex **2**, having dpq and dtdp ligands, is an efficient cleaver of DNA in air, forming a significant quantity of linear DNA. This complex, however, shows the formation of only NC DNA under an argon atmosphere, suggesting that one photosensitizer is inactive in anaerobic media. The dpq complex **4**, having a photoinactive azelate ligand, exhibits the formation of only NC DNA in the air and no DNA cleavage activity under argon. The cleavage data suggest that the dpq ligand bound to copper(II) is photoactive only under aerobic conditions, while dtdp is active under both aerobic and anaerobic media. The diamagnetic d^{10}-zinc(II) complex **5** does not show any significant DNA photocleavage activity. Copper(II) acetate hydrate and ligands H_2dtdp, dpq, phen, and azelaic acid (H_2az) alone do not show any apparent DNA photocleavage activity (lanes 2−5, Figure 5). A 5.0 μM solution of the phen complex **1** forms 81% of NC DNA upon irradiation at 365 nm for 2 h in the air (lane 12, Figure 5). Interestingly, it shows similar cleavage activity with 80% NC DNA formation when photoirradiation is done under argon (lane 7, Figure 5). The disulfide ligand in **1** seems to be the photosensitizer, while phen acts as a DNA binder. A 5.0 μM complex **2** shows 91% DNA cleavage with the formation of 30% linear DNA at 365 nm in the air (lane 13, Figure 5). The same complex shows the formation of 89% of NC DNA under argon (lane 8, Figure 5). The azelate analogue **3**, lacking any photosensitizing ligand, is inactive in both UV and visible light.

A similar pattern of DNA cleavage activity has been observed for **1** and **2** in red light under both aerobic and anaerobic media. A 7.5 μM solution of the complex exhibits formation of 80−90% of NC DNA in 647.1 nm red light (lanes 4 and 10 in Figure 6). Both the dpq and dtdp ligands in **2** are photoactive in air, and only the dtdp ligand acts as a photosensitizer under argon. The dpq complex **4**, having the azelate ligand, shows efficient DNA photocleavage activity at 365 and 647.1 nm, forming the NC form of DNA in air. This complex is, however, photoinactive under an argon atmosphere. The dtdp complexes **1** and **2** show efficient DNA photocleavage activity, even at a longer wavelength of >750 nm in air and argon (lanes 7 and 8 in Figure 6). The results are important, as anaerobic photocleavage of DNA at >750 nm is unprecedented in the literature.[1] The DNA binding propensity of the copper(II) complexes has been studied using the DNA minor groove binder distamycin and major groove binder methyl green (lanes 13−16 in Figure 6; Figure S13, Supporting Informa-

(44) Veal, J. M.; Rill, R. L. *Biochemistry* **1991**, *30*, 1132.
(45) Satyanarayana, S.; Dabrowiak, J. C.; Chaires, J. B. *Biochemistry* **1993**, *32*, 2573.
(46) Wittung, P.; Nielsen, P.; Norden, B. *J. Am. Chem. Soc.* **1996**, *118*, 7049.

Table 3. Selected pUC19 DNA (30 μM) Cleavage Data for the Complexes **1**−**5**

		λ = 365 nm (t = 1 h)[a]		λ = 647.1 nm (t = 2 h)[a]	
serial no.	reaction condition[b]	%cleavage (air)	%cleavage (argon)	%cleavage (air)	%cleavage (argon)
1	DNA control	2	5	2	3
2	DNA + [{(phen)Cu}$_2$(μ-dtdp)$_2$] (**1**)	81	80	83	80
3	DNA + [{(dpq)Cu}$_2$(μ-dtdp)$_2$] (**2**)	91[c]	89	95[d]	89
4	DNA + [{(phen)Cu}$_2$(μ-az)$_2$] (**3**)	18	8	15	
5	DNA + [{(dpq)Cu}$_2$(μ-az)$_2$] (**4**)	75	13	67	13
6	DNA + [{(phen)Zn}$_2$(μ-dtdp)$_2$] (**5**)	21	7		

[a] t, exposure time. [b] Ligands dtdp, dpq, azelaic acid, or copper(II) acetate hydrate alone gave %DNA cleavages of 5−10% in air or argon. Complex concentration: 5 μM at 365 nm and 7.5 μM at 647.1 nm. Cleavage of SC DNA gives the nicked circular (NC) form of DNA, except for complex **2**, which shows the formation of linear DNA along with the NC form under aerobic conditions. [c] 34% linear DNA. [d] 30% linear DNA.

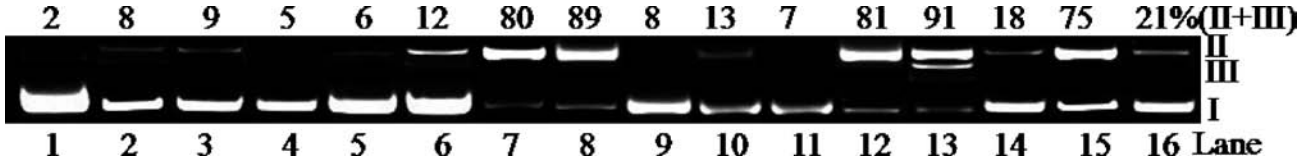

Figure 5. Cleavage of SC pUC19 DNA (0.2 μg, 30 μM) by complexes **1**−**5** (5 μM) in 50 mM Tris−HCl/NaCl buffer (pH, 7.2) on photoirradiation in 365 nm UV-A light for 1 h exposure time: lane 1, DNA control; lane 2, DNA + dtdp (10 μM); lane 3, DNA + dpq (10 μM); lane 4, DNA + copper(II) acetate hydrate (10 μM); lane 5, DNA + azelaic acid (10 μM); lane 6, DNA + **2** (in dark); lanes 7−11, DNA + complexes **1**−**5** (under argon); lanes 12−16, DNA + complexes **1**−**5** (in air) [lanes 1−6, in air].

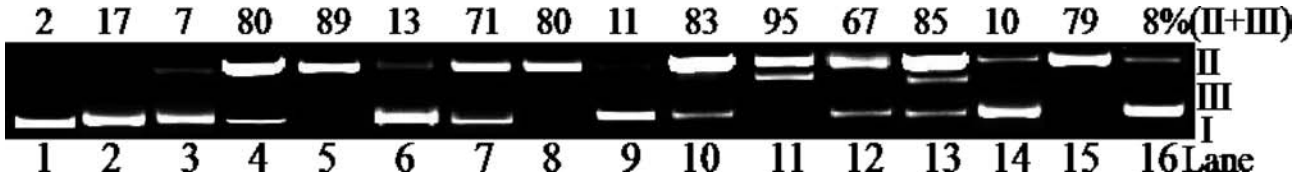

Figure 6. Cleavage of SC pUC19 DNA (0.2 μg, 30 μM) by complexes **1**, **2**, and **4** (7.5 μM) in 50 mM Tris−HCl/NaCl buffer (pH, 7.2) in 647.1 nm and >750 nm red light (100 mW) for an exposure time of 2 h: lane 1, DNA control (air); lane 2, DNA + distamycin (100 μM, 647.1 nm, air); lane 3, DNA + methyl green (200 μM, 647.1 nm, air); lanes 4−6, DNA + complexes **1**, **2**, and **4**, respectively (argon, 647.1 nm); lanes 7−9, DNA + complexes **1**, **2**, and **4**, respectively (argon, >750 nm); lanes 10−12, DNA + complexes **1**, **2**, and **4**, respectively (air, 647.1 nm); lane 13, DNA + distamycin + complex **2** (air, 647.1 nm); lane 14, DNA + methyl green + complex **2** (air, 647.1 nm); lane 15, DNA + distamycin + complex **1** (air, 647.1 nm); lane 16, DNA + methyl green + complex **1** (air, 647.1 nm).

tion). Complexes **1**−**4** show no inhibition in the DNA photocleavage activity upon addition of distamycin. In the presence of methyl green, complete inhibition in the DNA cleavage activity is observed. The cleavage data suggest a major groove-binding propensity of the complexes. The results are important, as the phen and dpq complexes of copper are known to be minor groove binders of DNA.[47−50] The experimental data suggest a major groove-binding preference along with partial intercalation to the base pairs. This could be possibly due to greater bulk of the binuclear complexes.

To explore the mechanistic aspects of the cleavage reactions in 365 nm UV-A light and 647.1 nm red light, DNA cleavage experiments have been carried out using the dtdp complexes in the presence of external reagents like sodium azide and L-histidine as singlet oxygen ($^1O_2$) quenchers, DMSO and catalase as hydroxyl radical (HO$^\bullet$) scavengers, and SOD as an $O_2^{\bullet-}$ radical scavenger. The reactions have also been carried out in D_2O, in which the lifetime of $^1O_2$ is known to be significantly higher than that in water.[51,52] A

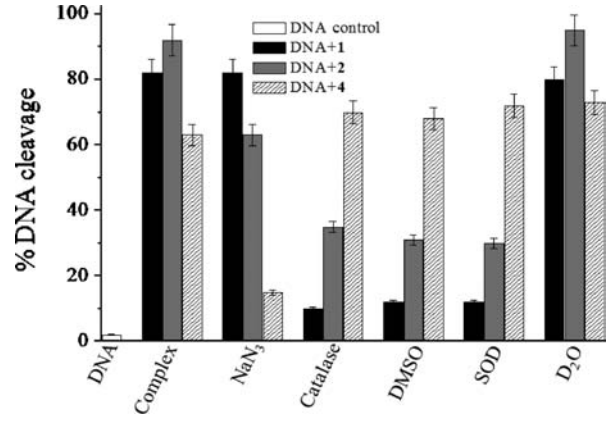

Figure 7. Bar diagram on the cleavage of SC pUC19 DNA (30 μM) by [{(phen)Cu}$_2$(μ-dtdp)$_2$] (**1**), [{(dpq)Cu}$_2$(μ-dtdp)$_2$] (**2**), and [{(dpq)Cu}$_2$(μ-az)$_2$] (**4**) (5.0 μM, 1 h) in the presence of various additives on photoirradiation at 365 nm in 50 mM Tris−HCl/NaCl buffer (pH, 7.2) [NaN_3, 100 μM; catalase, four units; DMSO, 4 μL; SOD, four units].

significant inhibition of the DNA photocleavage is observed for complex **1** in the presence of catalase, DMSO, and SOD, suggesting the involvement of hydroxyl or superoxide radicals in the DNA photocleavage under aerobic conditions (Figure 7, Figure S13, Supporting Information). No apparent inhibition of DNA photocleavage activity is observed in the presence of NaN_3 and L-histidine. The addition of D_2O shows no apparent effect on the DNA cleavage activity. The results exclude the singlet oxygen ($^1O_2$, $^1\Delta_g$) pathway in the DNA photocleavage reaction at 365 and 647.1 nm for **1**. Complex

(47) Sigman, D. S. *Acc. Chem. Res.* **1986**, *19*, 180.
(48) Erkkila, K. E.; Odom, D. T.; Barton, J. K. *Chem. Rev.* **1999**, *99*, 2777.
(49) Roy, M.; Pathak, B.; Patra, A. K. P.; Jemmis, E. D.; Nethaji, M.; Chakravarty, A. R. *Inorg. Chem.* **2007**, *46*, 11122.
(50) Dhar, S.; Senapati, D.; Das, P. K.; Chattopadhyay, P.; Nethaji, M.; Chakravarty, A. R. *J. Am. Chem. Soc.* **2003**, *125*, 12118.
(51) Khan, A. U. *J. Phys. Chem.* **1976**, *80*, 2219.
(52) Tapley, D. W.; Buettner, G. R.; Shick, J. M. *Biol. Bull.* **1999**, *196*, 52.

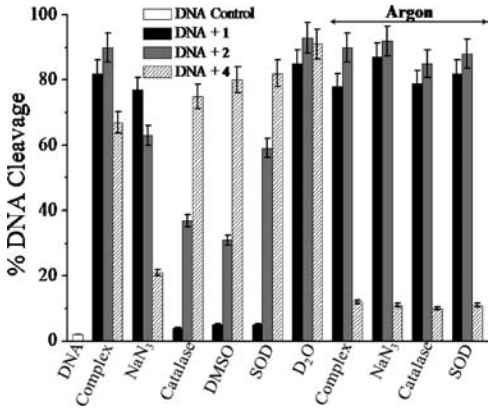

Figure 8. Bar diagram showing the extent of cleavage of SC pUC19 DNA (30 μM) by [{(phen)Cu}$_2$(μ-dtdp)$_2$] (**1**), [{(dpq)Cu}$_2$(μ-dtdp)$_2$] (**2**), and [{(dpq)Cu}$_2$(μ-az)$_2$] (**4**) (7.5 μM, 2 h) in the presence of various additives on photoirradiation in red light of 647.1 nm in 50 mM Tris−HCl/NaCl buffer (pH, 7.2) under both aerobic and anaerobic conditions [NaN_3, 100 μM; catalase, four units; DMSO, 4 μL; SOD, four units].

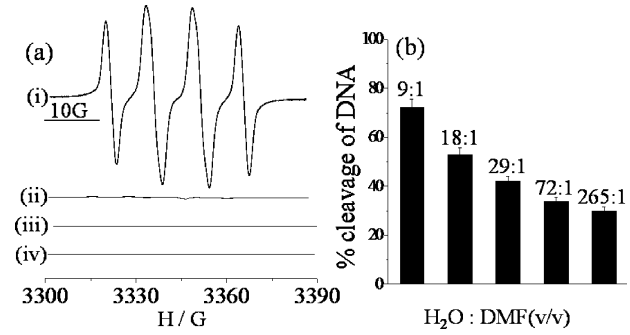

Figure 9. (a) EPR spectra of [{(phen)Cu}$_2$(μ-dtdp)$_2$] (**1**; 0.1 M) with 5,5-dimethyl-1-pyrroline N-oxide (DMPO, 0.04 M) in DMF−Tris−HCl buffer (1:1 v/v) after photoirradiation at >750 nm (i), [{(phen)Cu}$_2$(μ-az)$_2$] (**3**; 0.1 M) with DMPO (0.04 M) in DMF−Tris−HCl buffer (1:1 v/v) after photoirradiation at >750 nm (ii), DMPO (0.04 M) in DMF−Tris−HCl buffer (1:1 v/v) after photoirradiation at >750 nm (iii), and [{(phen)Zn}$_2$(μ-dtdp)$_2$] (**5**; 0.1 M) with DMPO (0.04 M) in DMF−Tris−HCl buffer (1:1 v/v) after photoirradiation at >750 nm (iv). (b) Cleavage of SC pUC19 DNA (30 μM) by [{(phen)Cu}$_2$(μ-dtdp)$_2$] (**1**; 7.5 μM, 2 h exposure) under anaerobic conditions on photoirradiation at >750 nm in 50 mM Tris−HCl/NaCl buffer (pH, 7.2) with varying DMF/H_2O (v/v) solvent ratios.

2 under aerobic conditions shows partial inhibition by the singlet oxygen quenchers and the hydroxyl radical scavengers (Figure 7, Figure S13, Supporting Information). An enhancement of DNA cleavage activity is observed in D_2O. The DNA cleavage data on **2** in air indicate that the copper(II)-bound dpq and dtdp ligands follow the $^1O_2$ (type-II) and HO$^\bullet$ pathways, respectively. This is supported by the fact that the dpq complex **4**, having the azelate ligand, shows inhibition with only singlet oxygen quenchers and enhancement of DNA cleavage in D_2O. The hydroxyl radical scavengers show no inhibitory effect for complex **4**. In summary, the aerobic DNA photocleavage by the dicopper(II) complexes involves the hydroxyl radical pathway for the disulfide moiety in dtdp and the singlet oxygen (type-II) pathway for the quinoxaline moiety of dpq.[53]

The mechanistic pathway for the dpq complex **2** of dtdp has been probed under anaerobic reaction conditions using argon (Figure 8, Figure S14, Supporting Information). It has been observed that singlet oxygen quenchers and hydroxyl radical scavengers have no apparent effect on the DNA cleavage activity in red light. The DNA photocleavage reaction under argon does not involve any ROS. We propose the involvement of dtdp ligand forming cleavage-active species in a type-I pathway. We have probed the effect of solvent on the DNA cleavage activity. It is observed that an increase in the concentration of DMF in the DMF−Tris buffer mixture increases the DNA photocleavage activity (Figure 9, Figure S15, Supporting Information).[17] Complex **1** alone, when exposed to >750 nm red light under argon in the presence of DMPO, gives a four-line X-band EPR spectrum in the DMF−Tris buffer (1:1 v/v) medium showing $a_N = 16.45$ and $a_H = 16.25$ G (Figure 9). The values compare well with the reported $a_N = 16.09$ and $a_H = 16.19$ G for the sulfide anion radical RS$^{\bullet-}$.[54] We propose the formation of the sulfide anion radical under argon as the active species cleaving DNA in a type-I process. In air, it presumably reacts with the dissolved oxygen in the solvent to produce a superoxide radical ($O_2^{\bullet-}$) that subsequently generates a hydroxyl radical.[17] The anaerobic DNA cleavage by the sulfide anion radical (RS$^{\bullet-}$) is speculated to proceed via formation of a nucleobase radical anion (B$^{\bullet-}$) that could activate the sugar moiety by hydrogen abstraction, leading to DNA cleavage.[7] The reactions involving the copper(II) complexes seem to be metal-assisted and involve metal-based charge-transfer and ligand field transitions. The zinc(II) complex is photoinactive in red light in the absence of any ligand field band. The dtdp copper(II) complexes having DNA binding phenanthroline bases are found to be significantly better DNA photocleavers under both aerobic and anaerobic reaction conditions than their binary [Cu(RSSR)]$_2$ analogue.[23,24]

Computational Studies. We have done computational studies to understand the following major experimental findings: (i) DNA major groove binding of the dicopper(II) complexes having phenanthroline bases as terminal ligands in preference to minor groove binding, (ii) complex **2** having dtdp and dpq ligands, showing photoinduced DNA double-strand breaks in air and single-strand nicks under argon, and (iii) red-light-induced anaerobic DNA cleavage activity of the copper(II) complexes of the dtdp ligand. DNA docking calculations carried out on [{(dpq)Cu}$_2$(μ-dtdp)$_2$] (**2**) with the d(CGCGAATTCGCG)$_2$ dodecamer (PBD ID: 355D) provide an energetically favorable docked pose that is shown in Figure 10 (Figure S16, Supporting Information). The complex binds at the major groove of ds DNA in preference to the minor groove. A minor groove approach of the binuclear complex leads to steric clash between the copper atom of the complex and the oxygen atom of the phosphate backbone of DNA. Experimental DNA cleavage data using minor groove binder distamycin and major groove binder methyl green also support major groove binding of the complexes. The DNA major groove binding involves the sulfur atom of dtdp, showing hydrogen-bonding interactions with the DNA base belonging to one of the strands [S4

(53) (a) Dhar, S.; Nethaji, M.; Chakravarty, A. R. *Inorg. Chem.* **2006**, *45*, 11043. (b) Dhar, S.; Senapati, D.; Reddy, P. A. N.; Das, P. K.; Chakravarty, A. R. *Chem. Commun.* **2003**, 2452.

(54) Bilski, P.; Chignell, C. F.; Szychlinski, J.; Borkowski, A.; Oleksy, E.; Reszka, K. *J. Am. Chem. Soc.* **1992**, *114*, 549.

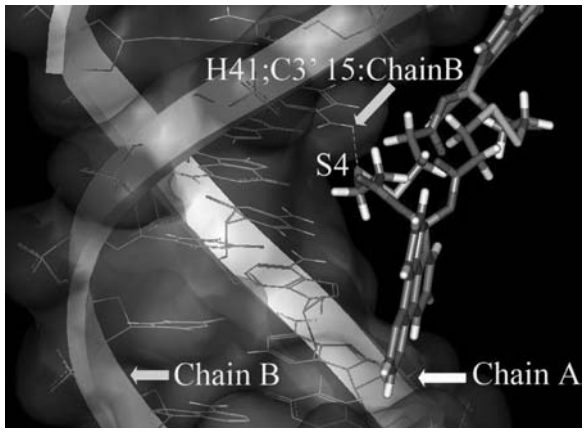

Figure 10. Docked state of [{(dpq)Cu}$_2$(μ-dtdp)$_2$] (**2**) showing chemically significant hydrogen-bonding interactions with d(CGCGAATTCGCG)$_2$ dodecamer (PDB ID: 355D).

Scheme 1. Probable Mechanistic Pathways Followed by the Ternary Complexes in the Photo-Induced DNA Cleavage Reactions under Aerobic and Anaerobic Conditions

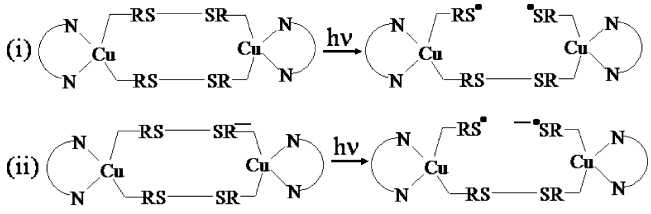

(complex **2**)···H41; Cyt15 (DNA chain-B), 2.60 Å] and the other strand being far apart from the sulfur atom. Such a binding pose also brings the dpq ligand close to chain A, making this complementary strand susceptible to cleavage under aerobic conditions.

DFT calculations have been done to understand the sulfur radical anion formation of complex **1**. The scission of the S−S bond in RS−SR (dtdp) can occur upon photoexcitation to give the radical RS$^{\bullet}$ or the anion radical species RS$^{\bullet-}$ (Scheme 1). The S−S bond dissociation energy (BDE) of the dtdp ligand is calculated to be 51.7 kcal M^{-1} (B3LYP/6-31G*, full optimization) by taking the energy difference of the reactants and products. The S−S BDE of the dtdp ligand in **1** is estimated to be 54.2 kcal M^{-1}. These values are quite high as compared to the energy of the 750 nm red light (38.4 kcal M^{-1}) used for the DNA cleavage. The BDE of the S−S bond is found to be reduced by the formation of radical anions as the electron goes to the antibonding S−S orbital.[41] Formation of sulfur radical anions is reported in the pulse radiolysis of cystine, cysteamine, hydrogen sulfide, and mercaptans.[55] The disulfide bond activation plays an important role in the physiological activity of rhodopsins.[56] The BDE estimations of the radical anion are 29.7 and 31.1 kcal M^{-1} for dtdp and complex **1**, respectively. The LUMO of **1** is a π* orbital concentrated on the phen ring, and the electron goes to this orbital upon reduction (Figure S17, Supporting Information). The electron is transferred to the S−S bond by a metal-assisted electron-transfer process that reduces the S−S bond strength. Photoexposure of the complex to 750 nm red light results in the cleavage of the S−S bond and formation of the sulfur anion radical that cleaves DNA. Although we have not done an exhaustive computational mechanistic study, our preliminary results show the important role of the copper atom in the electron-transfer process since the cleavage does not happen for the zinc(II) complex **5**.

Conclusions

Binuclear copper(II) complexes having DNA binding phenanthroline bases and dicarboxylates having a disulfide moiety show anaerobic DNA cleavage activity in red light. Complex **2**, having two photosensitizing moieties, namely, the quinoxaline ring of dpq and the disulfide of dtdp, shows DNA double-strand breaks in air following singlet oxygen and hydroxyl radical cleavage pathways. This complex cleaves DNA under argon, possibly involving sulfide anion radical species, thus making it a versatile DNA photocleaving agent in the PDT window under aerobic and hypoxic conditions. The disulfide ligand plays an important role in showing the anaerobic photocleavage of DNA since the analogous azelate complexes are inactive under similar conditions. The DNA photocleavage activity in >750 nm red light under argon makes complexes **1** and **2** unique in the PDT chemistry. Macrocyclic organic PDT drugs like lutetium texaphyrin (LUTRIN) and phthalocyanin-based compounds are known to be photoactive at near-IR wavelengths, but only under aerobic conditions.[14,15] We have recently reported oxovanadium(IV) complexes showing photoinduced DNA cleavage activity at >750 nm under aerobic conditions.[57] Conventional PDT requires simultaneously all three components, namely, light, oxygen, and a photosensitizer. This process becomes inefficient under hypoxic conditions. The present results are thus of importance toward designing and developing the chemistry of metal-based photosensitizers-cum-DNA binders for cellular application in PDT under hypoxic conditions.

Acknowledgment. We thank the Department of Science and Technology (DST, SR/S5/MBD-02/2007) and Department of Biotechnology, Government of India, for financial support and DST for the CCD diffractometer facility. We also thank Prof. E. D. Jemmis of the Department of Inorganic and Physical Chemistry and Prof. S. V. Bhat of the Department of Physics, Indian Institute of Science, Bangalore, for providing help in computational study and for the EPR spectral data. We are thankful to the Alexander von Humboldt Foundation, Germany, for the donation of an electroanalytical system and our Supercomputer Education and Research Center (SERC) for providing the computational facility. O.S., T.B., B.P. and A.K.P. are thankful to the Council of Scientific Industrial Research (CSIR, New Delhi) for research fellowships.

(55) (a) Mezyk, S. P. *Chem. Phys. Lett.* **1995**, *235*, 89. (b) Karmann, W.; Meissner, G.; Henglein, A. *Z. Naturforsch.* **1967**, *B22*, 273. (c) Karmann, W.; Granzow, A.; Meissner, G.; Henglien, A. *Int. J. Radiat. Phys. Chem* **1969**, *1*, 395.

(56) Shieh, T.; Han, M.; Sakmar, T. P.; Smith, S. O. *J. Mol. Biol.* **1997**, *269*, 373.

Supporting Information Available: Figures on mass spectra, unit cell packing, electronic spectral data, cyclic voltammetric data, magnetic susceptibility, DNA binding, cleavage, and mechanistic and theoretical data (Figures S1−S17). Selected bond distances and angles for **1**·$2H_2O$ (Table S1) and tables listing the crystallographic data, atomic coordinates, complete bond distances and angles, anisotropic thermal parameters, and hydrogen atom coordinates for the complex **1**·$2H_2O$ (CIF). This material is available free of charge via the Internet at http://pubs.acs.org.

IC800806J

(57) Sasmal, P. K.; Patra, A. K.; Nethaji, M.; Chakravarty, A. R. *Inorg. Chem.* **2007**, *46*, 11112.